



# Modified structural characteristics and enhanced electrochemical properties of oxygen-deficient $\text{Li}_2\text{MnO}_{3.8}$ obtained from pristine $\text{Li}_2\text{MnO}_3$



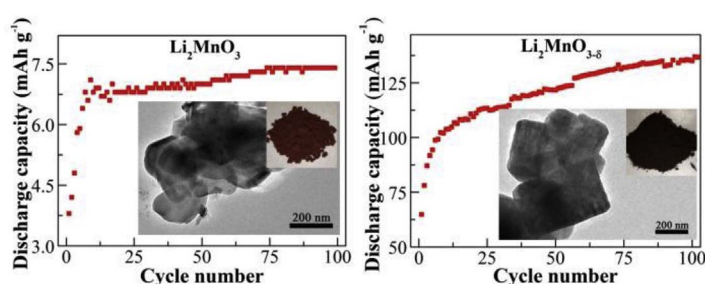
Xiao Tan, Rui Liu, Congxin Xie, Qiang Shen\*

Key Laboratory for Colloid and Interface Chemistry of Education Ministry, School of Chemistry and Chemical Engineering, Shandong University, Jinan 250100, China

## HIGHLIGHTS

- $\text{Li}_2\text{MnO}_{3.8}$  is obtained from  $\text{Li}_2\text{MnO}_3$  by the  $\text{NaBH}_4$ -assisted heat-treatment at 380 °C.
- The modified structural properties of oxygen-deficient  $\text{Li}_2\text{MnO}_{3.8}$  are obvious.
- The reversible capacity of  $\text{Li}_2\text{MnO}_{3.8}$  is ca. 20 times as large as that of  $\text{Li}_2\text{MnO}_3$ .
- Gradual electrochemical activations of  $\text{Li}_2\text{MnO}_3$  and  $\text{Li}_2\text{MnO}_{3.8}$  are almost the same.
- A cationic-anionic redox mechanism explains the gradual activation of  $\text{Li}_2\text{MnO}_{3.8}$ .

## GRAPHICAL ABSTRACT



## ARTICLE INFO

### Keywords:

Lithium-rich manganese(IV) oxide  $\text{Li}_2\text{MnO}_3$   
Oxygen-deficient  $\text{Li}_2\text{MnO}_{3.8}$   
Sodium borohydride  $\text{NaBH}_4$   
Electrochemical activation  
Lithium-ion batteries

## ABSTRACT

Lithium-rich manganese(IV) oxide  $\text{Li}_2\text{MnO}_3$  has hardly any activity as the cathode active substance of lithium-ion batteries (LIBs) but its reversible capacity can be greatly improved by introducing oxygen deficiencies. After the solid-state heat treatment of nanocrystalline  $\text{Li}_2\text{MnO}_3$  by sodium borohydride ( $\text{NaBH}_4$ ), the resulting  $\text{Li}_2\text{MnO}_{3.8}$  crystallites comparatively acquire distinguishable appearances in color and shape and slight differences in surface composition and lattice structure. As a LIB cathode within the potential range of 2.5–4.7 V, at 20  $\text{mA g}^{-1}$  pristine  $\text{Li}_2\text{MnO}_3$  gives the specific discharge capacities of 3.3, 5.0 and 7.4  $\text{mAh g}^{-1}$  in the 1st, 10th and 100th cycles, while the derivative  $\text{Li}_2\text{MnO}_{3.8}$  delivers the relatively high values of 64.8, 103.8 and 140.2  $\text{mAh g}^{-1}$  in the 1st, 10th and 120th cycles, respectively. Aside from the similar phenomenon of gradual electrochemical activation, substituting  $\text{Li}_2\text{MnO}_{3.8}$  for  $\text{Li}_2\text{MnO}_3$  means the great enhancements of charge-transfer ability and electrochemical performances. Especially, the cationic-anionic redox mechanisms of  $\text{Li}_2\text{MnO}_3$  and  $\text{Li}_2\text{MnO}_{3.8}$  are similar to each other, suggesting a possible solution to prepare high-performance  $x\text{Li}_2\text{MnO}_{3.8}(1-x)\text{LiMO}_2$  solid solutions for application purposes.

## 1. Introduction

Cathode materials with high capacity, low cost and long lifespan play an important role in their commercialization for lithium-ion batteries (LIBs) [1–3]. Ever since the demonstration of lithium-rich

manganese-based layered oxides or solid solutions,  $x\text{Li}_2\text{MnO}_3(1-x)\text{LiMO}_2$  (e.g.,  $M = \text{Ni}_{1/3}\text{Co}_{1/3}\text{Mn}_{1/3}$ ), for next generation high-capacity LIB cathodes [4–6], their electrochemically “inert” constituent  $\text{Li}_2\text{MnO}_3$ , with a low reversible capacity and/or a poor long-term cycling, has been regarded as an ideal model to investigate structural and

\* Corresponding author.

E-mail address: [qshen@sdu.edu.cn](mailto:qshen@sdu.edu.cn) (Q. Shen).

electrochemical properties of the lithium-rich layered compounds. This is simply due to the fact that, similar to the formula of “active” component  $\text{LiMO}_2$ , component  $\text{Li}_2\text{MnO}_3$  can also be re-written as  $\text{Li}[\text{Li}_{1/3}\text{Mn}_{2/3}]\text{O}_2$  to describe the additional lithium occupation in transition metal layers. However, this lithium arrangement can cause both phase transition and loss of reversible capacity during galvanostatic charge-discharge cycling. Therefore, if component  $\text{Li}_2\text{MnO}_3$  merely functionalizes to stabilize lattice structure of the active component  $\text{Li}[\text{Ni}_{1/3}\text{Co}_{1/3}\text{Mn}_{1/3}]\text{O}_2$ , with a theoretical capacity of  $\sim 280 \text{ mAh g}^{-1}$  for one-electron transfer, the well-known high-capacity feature of a solid solution  $0.5\text{Li}_2\text{MnO}_3 \cdot 0.5\text{Li}[\text{Ni}_{1/3}\text{Co}_{1/3}\text{Mn}_{1/3}]\text{O}_2$ , with an actual capacity higher than  $200 \text{ mAh g}^{-1}$ , is extremely difficult to understand, especially at a cut-off voltage lower than  $4.5 \text{ V}$ .

Well-crystallized  $\text{Li}_2\text{MnO}_3$  has a high theoretical capacity of  $459 \text{ mAh g}^{-1}$  calculated according to a fictitious two-electron transfer mechanism. Considering the nearly “inert” nature of  $\text{Li}_2\text{MnO}_3$  in practice, two well-recognized aspects should be mentioned: (i) further oxidation of  $\text{Mn}^{4+}$  in the octahedral coordination of  $\text{Li}_2\text{MnO}_3$  could hardly proceed even within the electrochemical window of  $2.5\text{--}4.8 \text{ V}$ , and (ii) origin of the limited capacity of  $\text{Li}_2\text{MnO}_3$  (i.e.,  $< 20 \text{ mAh g}^{-1}$ ) is still a controversial issue so far. Robertson and Bruce attribute the low electrochemical activity to the ion-exchanging of  $\text{Li}_2\text{MnO}_3$ -intercalated  $\text{Li}^+$  with electrolyte-generated  $\text{H}^+$ , while Komaba et al. explain the limited capacity contribution using the electrochemical redox reaction of gaseous  $\text{O}_2$  occurring at  $4.5 \text{ V}$  on  $\text{Li}_2\text{MnO}_3$  electrode surface [7,8].

Comparing to  $\text{Li}_2\text{MnO}_3$ , LIB cathode material  $\text{Li}_4\text{Mn}_2\text{O}_5$  possesses a high electrochemical activity and displays a discharge capacity as high as  $355 \text{ mAh g}^{-1}$ , assigned to the combined contributions of  $\text{Mn}^{3+}/\text{Mn}^{4+}$ ,  $\text{Mn}^{4+}/\text{Mn}^{5+}$  and  $\text{O}^{2-}/\text{O}^-$  redox couples [9]. In formula  $\text{Li}_2\text{MnO}_3$ , the partially replacing of  $\text{Mn}^{4+}$  with  $\text{Ru}^{4+}$  successfully induces the formation of oxygen deficiencies and thus the electrochemical redox reactions of  $\text{Mn}^{3+}/\text{Mn}^{4+}$ ,  $\text{Ru}^{4+}/\text{Ru}^{5+}$  and  $\text{O}^{2-}/\text{O}^-$  couples could account for the high reversible capacity (i.e.,  $220 \text{ mAh g}^{-1}$ ) of modified  $\text{Li}_2\text{Ru}_{1-y}\text{Mn}_y\text{O}_3$  cathodes reasonably [10]. Similarly,  $\text{Li}_2\text{MnO}_3$ -like compounds such as  $\text{Li}_2\text{Ru}_{1-y}\text{Sn}_y\text{O}_3$ ,  $\text{Li}_2\text{Ru}_{1-y}\text{Ti}_y\text{O}_3$  and  $\text{Li}_2\text{IrO}_3$  have been further proved to endow with both cationic  $\text{M}^{n+}$  and anionic  $\text{O}_2^{n-}$  redox activities for their high-capacity characteristics [11–13].

Differing with Tarascon's designs of  $\text{Li}_2\text{MnO}_3$ -like compounds [11–13], optimized synthesis or structural modification of pristine  $\text{Li}_2\text{MnO}_3$  should be mentioned, which relates to the generation of a commonly defined  $\text{Mn}^{3+}$ -doping and oxygen-deficient form (i.e.,  $\text{Li}_2\text{MnO}_{3-\delta}$ ) for the improvement of electrochemical activity. For example, after a low-temperature treatment of pristine  $\text{Li}_2\text{MnO}_3$  by metal hydride (i.e.,  $\text{CaH}_2$  or  $\text{LiH}$ ), the resulting oxygen-deficient  $\text{Li}_2\text{MnO}_{3-\delta}$  could deliver an extremely high initial discharge capacity of  $388 \text{ mAh g}^{-1}$  at  $10 \text{ mA g}^{-1}$  but its improvement of the cycling stability was urgently needed [14]. Another example is the oxygen-deficient structure obtained via carbonthermal reduction, which presented a good cycling stability of the cathode  $\text{Li}_2\text{MnO}_{3-\delta}$  but possessed a low specific capacity (e.g., 50th cycle,  $60 \text{ mAh g}^{-1}$ ,  $10 \text{ mA g}^{-1}$ ) in each cycle therein [15].

Generally, introducing oxygen vacancies can intrinsically improve the electron/ion conductivity and electrochemical performance of transition metal oxides [16–21], and aroused by this, in this paper solid-state sodium tetrahydroborate ( $\text{NaBH}_4$ ) was used as reducing agent to obtain the oxygen-deficient structure of  $\text{Li}_2\text{MnO}_{3-\delta}$  from pristine  $\text{Li}_2\text{MnO}_3$  via a thermal treatment route. Although acquiring a low discharge capacity of no more than  $7.4 \text{ mAh g}^{-1}$  at  $20 \text{ mA g}^{-1}$ , the gradual electrochemical activation of pristine  $\text{Li}_2\text{MnO}_3$  was detected. By comparison, the derived  $\text{Li}_2\text{MnO}_{3-\delta}$  has almost the same increasing trend of electrochemical activation, and its high reversible capacity and superior cycling performance (e.g.,  $140.2 \text{ mAh g}^{-1}$ ,  $20 \text{ mA g}^{-1}$ , 120th cycle) were investigated in detail in context.

## 2. Experimental

### 2.1. Syntheses of pristine $\text{Li}_2\text{MnO}_3$ and its derived $\text{Li}_2\text{MnO}_{3-\delta}$

All the chemicals are of analytical grade and were used without further purification. Ultrapure water ( $18.2 \text{ M}\Omega \text{ cm}$ ) was used throughout samples preparation.

Syntheses of pristine  $\text{Li}_2\text{MnO}_3$  and its derived  $\text{Li}_2\text{MnO}_{3-\delta}$  were described as below. Firstly, amorphous  $\text{MnO}_2$  boxes were freshly prepared according to our previous results [22], which was used as a starting material to react with solid-state lithium carbonate  $\text{Li}_2\text{CO}_3$  at the Li: Mn elemental molar ratio of 2.05: 1.00. Prior to the solid-state reaction,  $\text{MnO}_2$  and  $\text{Li}_2\text{CO}_3$  powders were mixed by mechanical milling in ethanol for 2 h and then dried at  $80 \text{ }^\circ\text{C}$  overnight. Secondly, the admixtures of  $\text{MnO}_2$  and  $\text{Li}_2\text{CO}_3$  were heated under air-atmosphere at  $800 \text{ }^\circ\text{C}$  for 8 h, resulting in pristine  $\text{Li}_2\text{MnO}_3$ . Thirdly, pristine  $\text{Li}_2\text{MnO}_3$  was thoroughly mixed with powdered sodium tetrahydroborate ( $\text{NaBH}_4$ ) at a mass ratio of 1: 2 by mechanical milling in ethanol for 2 h and dried at  $80 \text{ }^\circ\text{C}$  overnight, and then placed into a nitrogen-atmosphere tube furnace at  $380 \text{ }^\circ\text{C}$  for 6 h. After cooling down to room temperature naturally, the admixture was washed with methanol and water for the complete removal of impurities and then dried at  $80 \text{ }^\circ\text{C}$  overnight, resulting in the oxygen-deficient sample referred to as a chemical formula of  $\text{Li}_2\text{MnO}_{3-\delta}$ .

### 2.2. Structural characterization

The chemical compositions of as-prepared  $\text{Li}_2\text{MnO}_3$  and its derived  $\text{Li}_2\text{MnO}_{3-\delta}$  were determined using an inductively coupled plasma/atomic emission spectrometer (ICP/AES). X-ray diffraction (XRD) measurements were performed on a Rigaku D/max-2400 powder X-ray diffractometer with  $\text{Cu-K}\alpha$  radiation ( $40 \text{ kV}$ ,  $120 \text{ mA}$ ) and  $2\theta$  range of  $10\text{--}80^\circ$  ( $0.08^\circ$  step per 25 s), and program Xpert HighScore Plus 3 was used for X-ray Rietveld analyses. Raman spectra were recorded on a LABRAM-HR confocal laser micro-Raman spectrometer employing a  $20 \text{ mW}$  laser at  $632.8 \text{ nm}$ . Scanning electron microscopy (SEM) observation was conducted on a Hitachi SU8010, fitted with a field emission source and operating at an accelerating voltage of  $15 \text{ kV}$ . Low- or high-resolution transmission electron microscopy (TEM or HR TEM) and selected area electron diffraction (SAED) measurements were performed on a JEM 2100 microscope ( $200 \text{ kV}$ ). X-ray photoelectron spectroscopy (XPS) analyses were carried out using a VG ESCALAB 220i-XL UHV surface analysis system with a monochromatic Al  $\text{K}\alpha$  X-ray source.

### 2.3. Electrochemical characterization

Working electrodes were freshly prepared, described as below. At first, admixture of active substance (i.e.,  $\text{Li}_2\text{MnO}_3$  or  $\text{Li}_2\text{MnO}_{3-\delta}$ ;  $70 \text{ wt}\%$ ), acetylene black ( $20 \text{ wt}\%$ ) and polyvinylidene fluoride (PVDF;  $10 \text{ wt}\%$ ) were ground, followed by the addition of N-methylpyrrolidone to form uniform slurry. Then, the resulting slurry was cast onto an aluminum foil and dried at  $80 \text{ }^\circ\text{C}$  for 12 h in a vacuum desiccator. And then, the aluminum foil was cut into discs ( $12 \text{ mm}$  in diameter) and used as LIB cathodes. CR2032-type coin cells were assembled in an argon-filled glovebox, using metallic lithium, nickel foam, Celgard 2300 microporous membrane and commercial LBC 305-01  $\text{LiPF}_6$  solution as counter electrode, current collector, separator and electrolyte, respectively.

All the electrochemical experiments were performed at  $30 \text{ }^\circ\text{C}$ , and an electrochemical window of  $2.5\text{--}4.7 \text{ V}$  (vs.  $\text{Li}^+/\text{Li}$  and hereafter) was selected unless otherwise specified. Galvanostatic cycling tests were conducted on a LAND CT2001A battery system, and cyclic voltammetry (CV) tests were carried out on a LK 2005A electrochemical workstation at  $0.1 \text{ mV s}^{-1}$ . Electrochemical impedance spectroscopy (EIS) tests were measured using an EG&G PAR 273A electrochemical workstation

Download English Version:

<https://daneshyari.com/en/article/7726315>

Download Persian Version:

<https://daneshyari.com/article/7726315>

[Daneshyari.com](https://daneshyari.com)